

NUMERICAL MODELING OF INDUCTION HARDENING OF GEAR WHEELS MADE OF STEEL AMS 6419

Received – Primljeno: 2017-12-20

Accepted – Prihvaćeno: 2018-08-20

Preliminary Note – Prethodno priopćenje

Numerical modeling of induction hardening of gear wheels made of steel AMS 6419 (AISI 300M) was presented in the paper. In order to determine correct values of critical temperatures for investigated steel Time-Temperature-Austenitization (TTA) and Continuous-Cooling-Temperature (CCT) diagrams are measured. Mathematical model of the process is formulated and described. Exemplary results are presented. Final conclusions are formulated.

Key words: alloy steel, induction hardening, gear wheel, numerical modeling, hardness.

INTRODUCTION

Induction hardening is the advanced heat treatment process consisting of three consecutive stages: rapid induction heating, very short austenitization and finally intensive cooling. Often the austenitization stage could be neglected because of very short time (less than hundreds of milliseconds). The most popular way of the application is the induction surface hardening characterized by hardening of thin surface zone of the body only and keeping soft and unchanged its internal part. Surface induction hardening is mostly applied for axi-symmetric and flat bodies, but the paper concentrates on more rarely applied induction hardening of gear wheels. There are different induction surface hardening methods for gear wheels accordingly to requested patterns of hardness distribution [1]. Some examples of such patterns are presented in Figure 1. In the paper it concentrates on the spin hardening - simultaneous heating of the gear by encircled inductor and then immediate cooling.

It is realized in the consecutive dual frequency hardening system (CDFIH) characteristic for gear wheels with modulus $m < 6$ mm. The gear wheel is heated first by medium frequency inductor (MF) to the temperature of about 700 °C, being higher than the modified lower temperature $A_{c_{1m}}$. It means beginning of the austenite transformation. Then the gear wheel is heated by the high frequency inductor (HF) to the hardening temperature T_h guaranteed a completion of the homogenous austenite microstructure. The process is terminated by immediate spraying. Modelling of the process is complicated because of necessity to solve non-linear and transient coupled electromagnetic, temperature and hardness fields [2]. The paper concentrates on numerical modelling of induction hardening of gear wheels

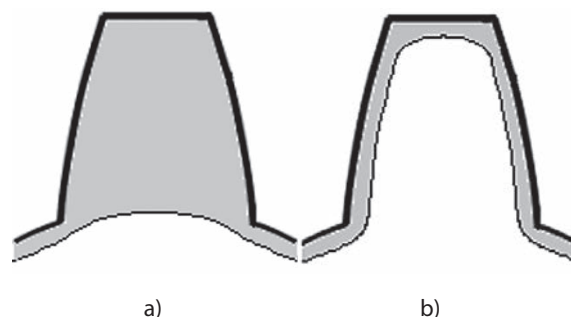


Figure 1 Profile of hardened zone a) through hardening, b) contour hardening

made of steel AMS 6419 (AISI 300M). Numerical modelling requires a correct identification of critical temperatures for the investigated steel. In order to determine them the TTA diagram was measured. Dependences of modified critical temperatures A_{c_m} , $A_{c_{3m}}$, $A_{c_{1m}}$ on velocity of induction heating v_{ih} are presented in Figure 2.

The critical temperature A_{c_m} guarantees completion of the homogenous austenite microstructure. For conventional, slow heating $A_{c_m} = 861$ °C. For fast induction heating the modified critical temperature A_{c_m} is distinctly bigger (for instance for $v_{ih} = 1\ 000$ K/s, $A_{c_m} = 1\ 065$ °C). Similar tendencies are observed for the mod-

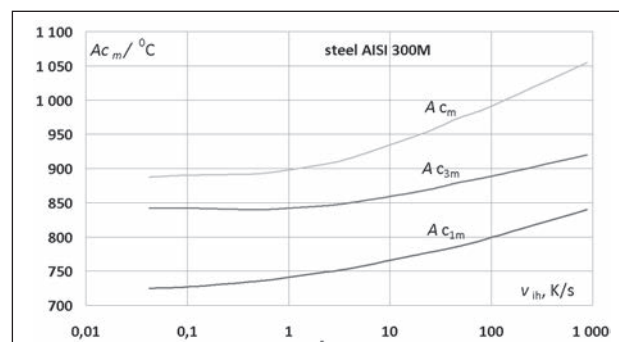


Figure 2 TTA diagram for steel AISI 300M (notations in text)

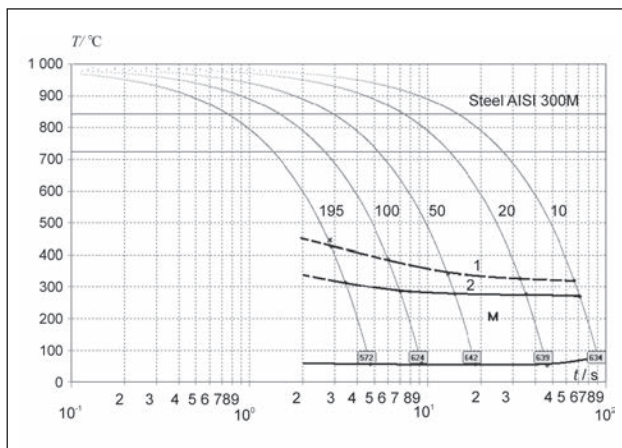


Figure 3 CTT diagram for steel AISI 300M
 1 – M_s , 2 – M_{s_f} , 3 – obtained hardness in Vickers degree, M – martensite, v_c – velocity of cooling.

ified lower critical temperature Ac_{1m} (beginning of austenite transformation) and the modified upper critical temperatures Ac_{3m} (termination of austenite transformation). Details are described for instance in [1]. The hardness distribution is determined based upon several CCT diagrams measured from different hardening temperatures in a range between ($T_h = 960...1050$ °C). Exemplary CCT diagram for the hardening temperature $T_h = 990$ °C is presented in Figure 3. Dependence of martensite start temperature M_s (line –) and martensite finish temperature M_{s_f} (line --) are depicted in Figure 3. If the final temperature after cooling are smaller than M_{s_f} and the velocity of cooling is big enough we obtained fully hardened martensite microstructure.

Even for small velocity of cooling ($v_c = 10$ K/s) expected value of hardness is achieved.

MATHEMATICAL MODEL

Mathematical model of the process is presented in Figure 4. At the beginning input data were completed (prior microstructure, material properties, configuration of the heating and cooling systems). Corresponding values of material properties: electric conductivity γ , thermal conductivity λ , specific heat c_p and magnetic permeability are temperature dependent. All these material properties data are taken from specialized databases or simply measured.

Induction heating stage is analyzed as coupled nonlinear electromagnetic and temperature problem. Based upon electromagnetic computations: module of the magnetic field intensity $|H|$, power density induced in the body p_v , and velocity of induction heating v_{ih} are determined. It makes possible to take into consideration the dependence of the magnetic permeability on the magnetic field intensity. Heat transfer coefficient α_{ch} for heating stage of the hardening represents both convection and radiation. It is supposed that the ambient temperature of convection and radiation environment equals to T_a is the same for both environments. Computation of induction heating terminates when the average

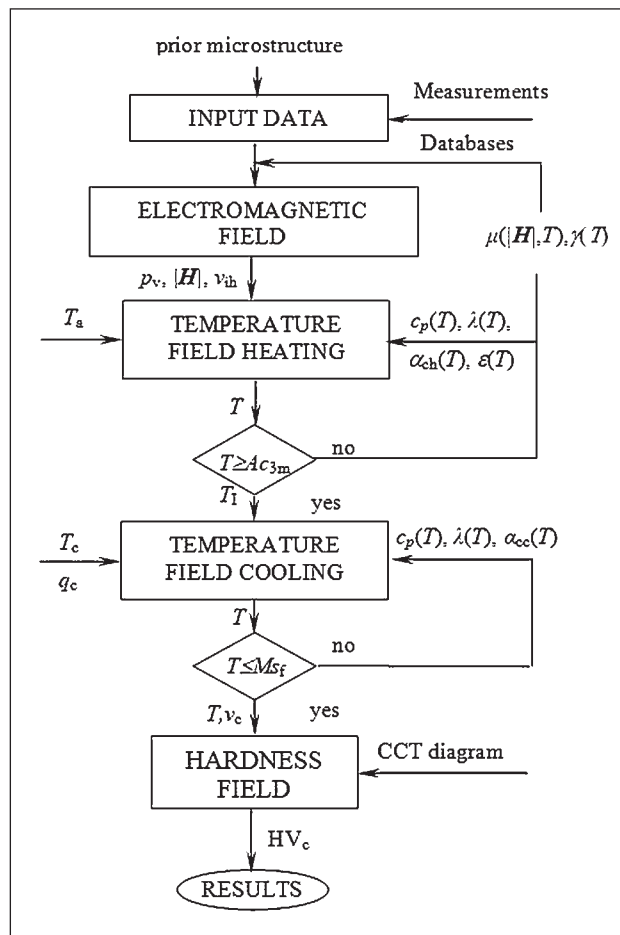


Figure 4 Mathematical model

temperature in the hardened zone reaches value of Ac_m which is dependent on velocity of induction heating. Then the nonstationary, nonlinear temperature field during cooling is determined. The temperature dependent heat transfer coefficient during cooling α_{cc} represents convection only. It is determined by measurements. Heat transfer between the body and quenchant depends on its temperature T_c and flow-rate q_c . This hardening stage is terminated when the average temperature at the working surface begins to be smaller than the M_{s_f} (Martensite Finish Temperature) which secures the full termination of the martensite transformation. Based upon the calculated velocity of cooling v_c the hardness and microstructure distributions within the body are determined by means of the measured Continuous Cooling Transformation (CCT) diagrams. At the end the calculated hardness distribution HV_c is compared with the experiments data HV_m and if the obtained accuracy tends to accepted value the final results are registered and printed.

ILLUSTRATIVE EXAMPLE

As the example the CDFIH process for gear wheels made of steel AISI 300M were analyzed. Basic parameters and dimensions of the induction hardening system were as follows:

Gear wheel: teeth number $n = 40$, width of the tooth ring $b = 0,007$ m, external diameter $d_e = 0,087$ m, internal diameter $d_i = 0,029$ m.

The gear wheel is heated first by the medium frequency (MF) inductor, next by the high frequency (HF) inductor and finally immediately cooled. Both inductors are have the same dimensions and they are equipped with the flux concentrator.

Inductor: number of coils $N = 1$, height of coil $h_1 = 0,007$ m, external diameter $D_{e1} = 0,109$ m, internal diameter $D_{i1} = 0,89$ m, flux concentrator Fluxtrol 50, density $\rho = 6100$ kg/m³, relative magnetic permeability $\mu_r = 36$, electric conductivity $\gamma = 0,2 \cdot 10^{-3}$ S/m, total height $h_c = 0,0205$ m, external diameter $D_e = 0,121$ m, internal diameter $D_i = 0,89$ m, thickness of upper and lower layers $\Delta h = 2 \times 0,005$ m.

Sprayer: distance between inductor and sprayer 0,0365 m, external diameter 0,1335 m, internal diameter 0,1235 m.

Heat transfer: convection heat transfer coefficient for heating $\alpha_{ch} = 20$ W/(m²K), quenchant: polymer solution Aqua Quench, its temperature $T_c = 30$ °C, flow-rate $q_c = 0,0001$ m³/s, concentration – 12%, convection heat transfer coefficient for cooling $\alpha_{cc} = 2000$ W/(m²·K).

Parameters: current $I_{MF} = 1\ 200$ A, heating time $t_{MF} = 3$ s, medium frequency $f = 30$ kHz, time between MF and HF heating $\Delta t = 0,1$ s, average temperature after MF heating 880 °C, current $I_{HF} = 200$ A, high frequency $f = 300$ kHz, heating time $t_{HF} = 0,2$ s, velocity of heating $v_{ih} \approx 300$ K/s, upper critical temperature $Ac_{3m} = 915$ °C, lower critical temperature $Ac_{1m} = 820$ °C, critical temperature $Ac_m = 1\ 020$ °C, time between heating and cooling: $\Delta t_{hc} = 0,1$ s, rotation velocity $v_r = 2$ r/s.

Let us consider temperature in five points depicted in Figure 5.

Results are shown in Figures 6 - 8

SUMMARY

Numerical modeling of the CDFIH process of gear wheels made of steel AISI 300M was discussed in the

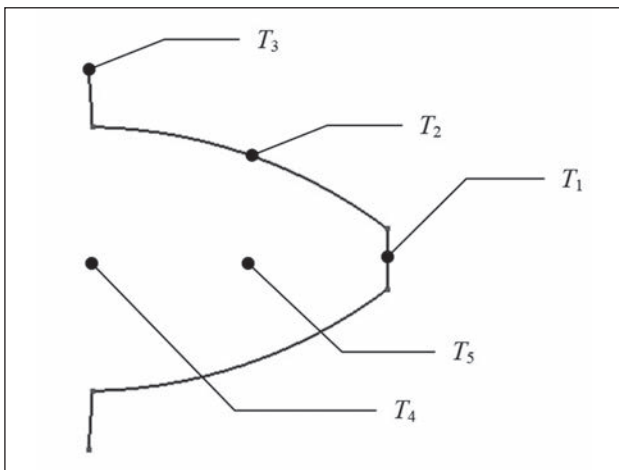


Figure 5 Location of measurement points T1 - T5

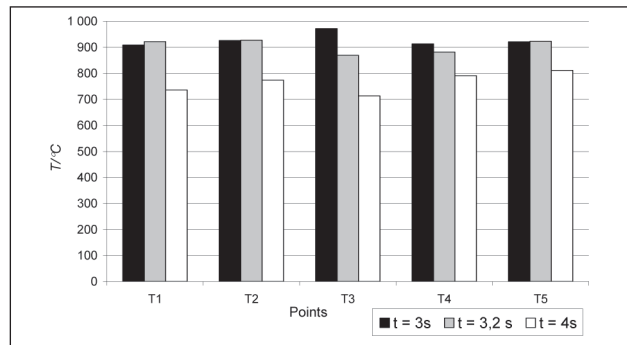


Figure 6 Temperature dependence on time for points T1 – T5

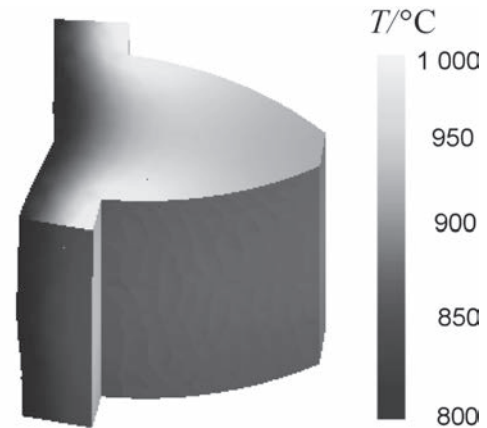


Figure 7 Temperature distribution after MF heating

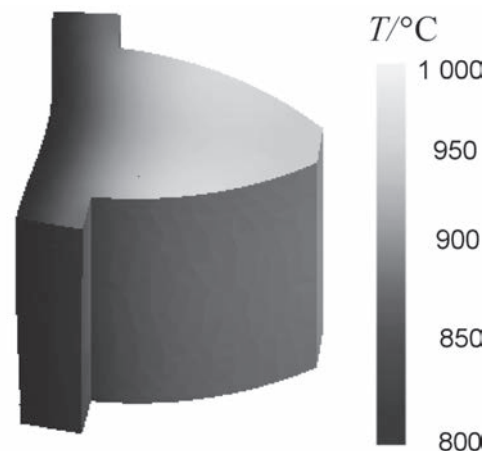


Figure 8 Temperature distribution after the HF heating

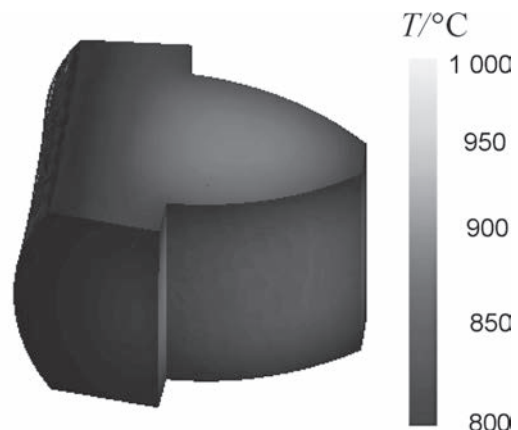


Figure 9 Temperature distribution at the beginning of cooling

paper. Mathematical model of the process is shortly described. Exemplary results for gear wheel with external diameter of 87 mm are presented. Computation of temperature distribution within the tooth makes possible to determine hardness and microstructure distribution. It was observed that for the investigated steel even small velocity of cooling could cause requested hardness distribution.

Acknowledgment

The paper was prepared within the NCBiR project PBS2/41/A5/2014

REFERENCES

- [1] V. Rudnev, G. Totten, *Induction Heating and Heat Treatment*, Materials Park, ASM International, 2014.
- [2] S. Lupi, *Fundamentals of Electroheat*. Electrical Technologies for Process Heating Springer, 2016.
- [3] M. Spezzaria, M. Forzan, F. Dughiero, *Multiphysical-multiscale FEM simulation of contour induction hardening of aeronautical gears*. Proceedings of the EPM conference, Cannes, 2015.
- [4] T. Wróbel, *The influence of inoculation type on structure of pure aluminium*, Proceedings of 21st International Conference on Metallurgy and Materials, 2012, pp. 1114-1120.
- [5] J. Barglik, *Induction hardening of steel elements with complex shapes*, *Przegląd Elektrotechniczny* 94 (2018) 4, 51-54.
- [6] J. Barglik, A. Smalcerz, *Influence of the magnetic permeability on modelling of induction surface hardening*. *Compel* 36, (2017), 2, 555-564.
- [7] E. Castellanos-Leal, D. Miranda, A. Coy, J. Barrero, J. González, O. Vesga-Rueda, *Induction hardening treatment and simulation for a grey cast iron used in engine cylinder liners*, *Journal of Physics* 786, (2017), 1-6.
- [8] A. Vieweg, G. Ressel, P. Prevedel, P. Raninger, M. Panzenböck, S. Marsoner, R. Ebner, *Induction hardening: Differences to a conventional heat treatment process and optimization of its parameters*, *Materials Science and Engineering* 119, (2016), 1-8.
- [9] A. Kohli, H. Singh, *Optimization of processing parameters in induction hardening using response surface methodology*, *Sadhana* 36, (2011), 2, 141-152.
- [10] M. Fisk, L.E. Lindgren, W. Datchary, V. Deshmukh, *Modelling of induction hardening in low alloy steels*, *Finite elements in analysis and design* 144, (2018), 61-75.

Note: Krajewska T. is responsible for English language, Katowice, Poland